9

Regular Article

Ramesha Kodandappa, Santhosh Nagaraja, Manjunatha Matnahalli Chowdappa, Manjunath Krishnappa, Gubbi Shivarathri Poornima, and Muhammad Imam Ammarullah*

Application of the Taguchi method and RSM for process parameter optimization in AWSJ machining of CFRP composite-based orthopedic implants

https://doi.org/10.1515/eng-2024-0057 received March 08, 2024; accepted June 01, 2024

Abstract: Abrasive water suspension jet (AWSJ) machining on carbon fiber-reinforced polymer (CFRP) composite-based orthopedic implants yielded insightful results based on experimental data and subsequent statistical validations. Underwater AWSJ cutting consistently outperformed free air cutting, with numerical findings demonstrating its superiority. For instance, at #100 abrasive size and 5 mm standoff distance (SOD), the material removal rate (MRR) peaked at 2.44 g/min with a kerf width of 0.89 mm and a surface roughness (SR) of 9.25 μm. Notably, the increase in abrasive size correlated with higher MRR values, such as achieving 2.15 g/min at #120 grit and 3 mm SOD. Furthermore, optimization

techniques like the Taguchi method and response surface methodology (RSM) were applied to refine machining parameters. These methodologies enhanced MRR, exemplified by achieving 2.10 g/min with #120 abrasive size and 5 mm SOD in underwater cutting conditions. The research explored the impact of key process parameters, namely, the speed, feed, and SOD on the MRR, kerf width, and SR in both free air cutting and underwater cutting conditions, which is one of the novel research endeavors in the domain of abrasive jet machining of composites.

Keywords: Taguchi method, response surface methodology, abrasive water suspension jet machining, carbon fiber-reinforced polymer composite, orthopedic implant

* Corresponding author: Muhammad Imam Ammarullah,

Department of Mechanical Engineering, Faculty of Engineering, Universitas Diponegoro, Semarang, 50275, Central Java, Indonesia; Undip Biomechanics Engineering & Research Centre (UBM-ERC), Universitas Diponegoro, Semarang, 50275, Central Java, Indonesia, e-mail: imamammarullah@gmail.com

Ramesha Kodandappa: Department of Mechanical and Automobile Engineering, School of Engineering and Technology, CHRIST (Deemed to be University), Bangalore, 560074, Karnataka, India

Santhosh Nagaraja: Department of Mechanical Engineering, MVJ College of Engineering, Bangalore, 560067, Karnataka, India Manjunatha Matnahalli Chowdappa: Department of Mechanical Engineering, Bangalore Institute of Technology, Bangalore, 560004, Karnataka, India

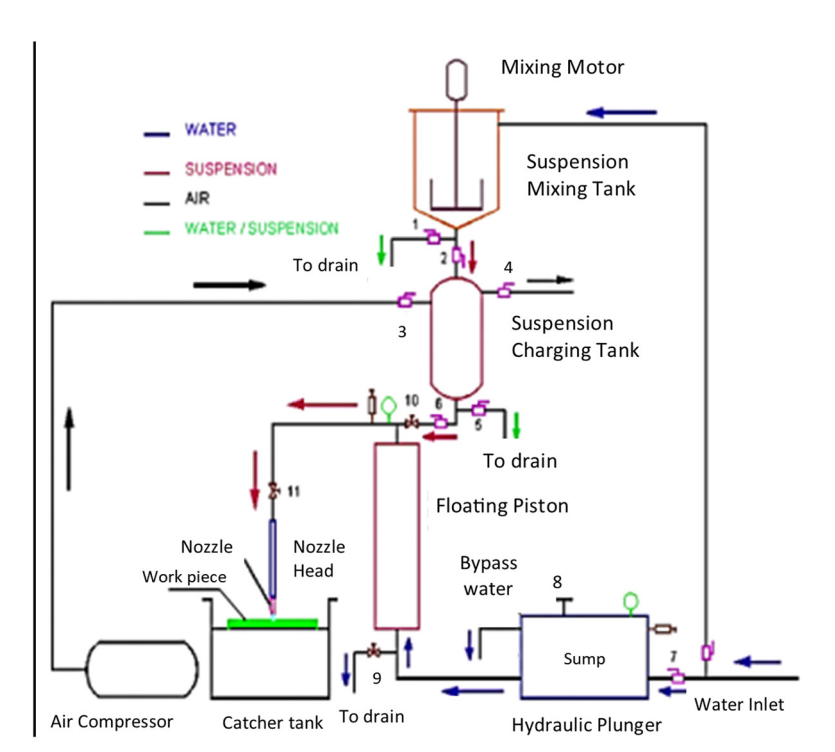
Manjunath Krishnappa: Department of Mechanical Engineering, S.E.A. College of Engineering and Technology, Bangalore, 560049, Karnataka, India

Gubbi Shivarathri Poornima: Department of Chemistry, New Horizon College of Engineering, Bangalore, 560103, Karnataka, India ORCID: Ramesha Kodandappa 0000-0002-3725-5563; Santhosh Nagaraja 0000-0002-3683-9356; Manjunatha Matnahalli Chowdappa 0000-0003-2242-8481; Manjunath Krishnappa 0009-0001-3993-7517; Gubbi Shivarathri Poornima 0000-0001-5824-2078; Muhammad Imam Ammarullah 0000-0002-8845-7202

1 Introduction

Carbon fiber-reinforced polymer (CFRP) composites renowned for their radiolucency, biocompatibility, reduced stress shielding, fatigue resistance, and corrosion resistance are attractive materials of choice for orthopedic implants. These materials offer a favorable combination of durability, rigidity, a high strength-to-weight ratio, and corrosion resistance [1]. However, machining these composites for application as orthopedic implants using conventional methods presents challenges due to their robust layers resulting in increased tool wear and the occurrence of splintering and delamination along the component edges. Such defects can significantly compromise the strength of the final components [2].

To address these issues, the abrasive water jet (AWJ) machining method has emerged as a promising non-conventional alternative. In AWJ machining, abrasive particles are mixed with a high-pressure, concentrated water jet. The sharp edges of these abrasive particles act as cutting edges, and the kinetic energy of the water—abrasive mixture removes the material through erosion. Despite its



- Mixing tank outlet valve
- 2. Suspension inlet to SCT
- 3. Air inlet to SCT
- 4. Air pressure relief valve
- 5. Outlet valve from SCT
- 6. Suspension charging valve
- 7. Water inlet to pump
- 8. Pressure Regulating valve
- 9. Water Outlet from FPC
- 10. Suspension Inlet to FPC
- 11. Nozzle needle valve

SCT: Suspension Charging/Storage Tank

FPC: Floating Piston Cylinder

Figure 1: Schematic of AWSJ machining.

advantages, AWJ machining faces challenges due to the uneven suspension of abrasive particles in water, leading to decreased cutting efficiency. An innovative solution to this challenge is abrasive water suspension jet (AWSJ) machining. This technique involves increasing the water viscosity by incorporating a polymer, such as zycoprint. This modification helps achieve a uniform distribution of abrasive particles in water, consequently enhancing the cutting efficiency [3]. Figure 1 shows the schematic diagram of AWSJ machining.

Despite the significance of CFRP composites in the biomedical industry, research on AWSI machining for these materials remains limited [4,5]. Existing studies primarily focused on exploring the impact of process parameters governing AWSI machining on the surface quality and associated defects like kerf width and surface roughness (SR) [6,7]. Ramulu et al. [8] carried out a series of experiments to investigate the impact of cutting parameters on kerf taper and SR in the AWSJ machining process of a glass fibre-reinforced plastic (GFRP) composite laminate. Mathematical models were formulated by the researchers to predict both the SR and kerf taper. Additionally, the researchers delved into factors contributing to the formation of striations on the cut surface. Wang [9] evolved a statistically designed principle model that was utilized to investigate the impact of jet angles on the production of high-quality cuts in the multidirectional cutting of ceramics through AWJ

machining. Additionally, a novel cutting head oscillation technique was implemented to improve the overall cut quality achieved by AWJ. The study revealed distinct characteristics in different zones of the cut. In the upper zone, the surface appeared smooth, devoid of visible striations and pits, with the kerf width tapering and reaching the minimum width at the end of this zone. Moving to the middle zone, noticeable striations were present, although pits were absent, and the kerf width remained consistent with that of the upper zone. Finally, in the lower zone, characterized by numerous pits, the kerf curvature exhibited a gradual change, and a pronounced ballooning formation was observed. Chen [10] accomplished the examination of cut surfaces across various materials through scanning electron microscopy and revealed that the formation of striations can be attributed to factors such as the presence of wavy abrasive particles, variations in kinetic energy distribution, fluctuations in the parameters of the AWJ process - namely, traverse speed, pressure, and abrasive flow rate as well as the influence of vibrations on both the workpiece and the nozzle traverse system.

Akkurt and Kulekci [11] carried out experiments to investigate the impact of both the feed rate and workpiece thickness on the deformation effect of varying workpiece thicknesses. The research aimed to assess the influence of deformation wear and cutting wear mechanisms on the resulting surface quality. The findings indicated that the

cutting wear mechanism yielded superior surface quality compared to the deformation wear mechanism. The study cautioned against cutting materials with thickness below a specified limit due to the adverse effects of high pressure on thinner materials. Azmir and Ahsan [12] conducted experiments on the SR and kerf taper ratio attributes of a GFRP composite laminate subjected to AWJ machining. They formulated an empirical model to assess the impact of machining parameters on the SR and kerf taper ratio. Their findings indicated that employing a harder abrasive material vielded superior machining characteristics. Furthermore, they observed that the higher hydraulic pressure and abrasive mass flow rate led to enhanced machining performance. Conversely, reducing the standoff distance (SOD) and traverse rate showed potential for improving machining characteristics. Nair and Kumanan [13] concentrated their efforts on optimizing the form and dimensions of a jet-drilled hole using grey relational analysis. They systematically analyzed the interactive effects of individual means for the selected experimental parameters. The findings validate that the abrasive mass flow rate, water jet pressure, and SOD have been successfully optimized. As a result, the machined surfaces of INCONEL alloy 617 demonstrate superior characteristics. Ravi Kumar et al. [14] successfully conducted a study on optimizing AWSI machining through the application of response surface methodology (RSM). This involved a detailed analysis of experimental trials and their outcomes, focusing on critical aspects and validations. Their efforts were directed toward optimizing machining parameters for abrasive jet machining of aluminum/tungsten carbide composites. The reported results indicate that the chosen optimum parameters not only enhance the material removal rate (MRR) but also reduce the SR by 22%. This improvement is attributed to the careful selection of appropriate SOD and traverse speed during the machining process. Deepak et al. [15] studied on the impact of abrasive grain size and nozzle diameter on composite SR; they observed a direct correlation between the SR, abrasive grain size, and nozzle diameter. This relationship is deemed crucial for achieving enhanced machinability in AWSJ machining. Anjaiah and Chincholkar [16] conducted a sequence of experiments aimed at investigating the impact of low-pressure AWJs on brittle materials. Their findings indicate a linear correlation between pressure increments and the enhancement of metal removal rates in brittle materials. Furthermore, they explored the influence of polymer liquid concentration on the MRR and determined that MRR rises proportionally with the higher percentages of polymer in the slurry. Brandt et al. [17] pioneered an AWSJ machining using the bypass principle, operating at pressures of up to 200 MPa. This setup involves storing a highly concentrated mixture of polymerized water and abrasives in

a water storage vessel. Subsequently, the mixture is loaded into the cutting system and pressurized onto the workpiece in the form of a fine jet to achieve precision cutting of the target material.

The AWSI machining system operates through a meticulous sequence of five stages. It commences with suspension preparation, where water is blended with zycoprint to increase the viscosity, followed by the addition of abrasive powder. The resulting mixture is transferred to a storage tank. Subsequently, the suspension is filled into the suspension charging tank, necessitating the closure of specific valves and the release of trapped air. Charging the floating piston cylinder involves a controlled process of opening valves to allow compressed air to fill the cylinder with suspension until the water flow ceases. The cutting operation ensues, with the suspension pressurized and expelled through a nozzle controlled by CNC, following safety protocols such as wearing protective gear and regulating pressure. Finally, the cleaning procedure involves flushing hoses with fresh water to prevent any residue buildup that could impede system functionality. Figure 1 gives the schematic of the AWSI machining setup used in the present work.

The existing body of literature reveals a prevailing trend in research, wherein investigations into AWSI machining involve positioning the workpiece above water. Furthermore, the optimization of machining characteristics has predominantly employed statistical methods other than Taguchi techniques [18,19]. Notably, the use of "above water" AWSI machining introduces a potential challenge, as air entrapment in the AWI may occur, leading to jet expansion and subsequent impacts on machining characteristics such as kerf width and SR. Recognizing these observations, the current research aims to yield groundbreaking results [20,21]. The focus is on expanding the possibilities for future work in this domain by employing Taguchi techniques for optimizing process parameters, facilitated by the utilization of "Minitab and Design Expert Software" for process optimization [22,23].

From the extensive review of literature findings, the research gap related to the optimization of factors that affect the AWSJ machining of CFRP composite-based orthopedic implants in free air and underwater conditions is identified and subsequently addressed from the current work. By analyzing numerical data, the research aims at optimizing the process parameters affecting the MRR, kerf width, and SR across various scenarios [24,25]. Notably, the research highlights the novelty of underwater cutting over free air cutting, showing that specific combinations of abrasive size, SOD, and feed rate result in the best outcomes. Furthermore, the research work focuses on the effectiveness of optimization methods like the Taguchi method and RSM in

improving MRR, offering valuable guidance for optimizing AWSJ machining processes for CFRP composite-based orthopedic implants. This systematic approach adopted in the present work ensures optimal parameter selection, contributing to the efficiency and effectiveness of AWSJ machining process to achieve sustainability.

2 Experimentations and statistical methods

The current experimental investigation employs CFRP composite-based orthopedic implants as the work material to assess the MRR, kerf width, and SR under both "free air and underwater cutting" conditions. The choice of CFRP composite-based orthopedic implants is primarily motivated by its brittle nature, which makes it well suited for AWSJ cutting. The workpiece dimensions considered for AWSJ machining are $75\,\mathrm{mm}\times50\,\mathrm{mm}\times6\,\mathrm{mm}$ fabricated using hand lay-up techniques.

The fabrication of the CFRP composite laminates involves utilizing hand lay-up techniques, where the matrix phase consists of EPOXY-ASC resin cured with HY951 hardener, and the reinforcement is sourced from ZOLTEK Corporation. The CFRP composite laminate fabrication involves the following steps.

- The surface is meticulously prepared, ensuring it is free from abrasions and dirt while maintaining complete flatness. Subsequently, a gel release coat is applied to facilitate the effortless release of CFRP composite laminates.
- 2. The matrix phase is formulated by combining the necessary amount of epoxy resin with the hardener in a weight ratio of 10:1. The mixture is then stirred thoroughly to ensure that the weight ratio of the fiber to the resin and hardener blend falls within the prescribed range of 40:60.
- Additionally, a resin-hardener mixture in the form of a thin film is spread over the release coat. Subsequently, polyacrylonitrile (PAN)-based carbon fibers are layered onto this surface, and a second substantial coat of EPOXY-ASC resin-hardener mixture is applied uniformly across the carbon fiber.
- 4. Intermittent rolling is performed on this layer, which is enveloped in a thin plastic film treated with wax to facilitate smooth removal. The rolling process is executed with consistent pressure to ensure proper penetration.
- Afterward, eight additional layers of reinforcements and matrix are applied successively until a laminate in the range of 3.9–4.1 mm thickness is achieved for subjecting it to AWSJ machining in free air and underwater cutting conditions.
- 6. To achieve the desired surface finish, a thin layer of a resin and hardener mixture is carefully applied.

7. The CFRP composite laminate is subsequently allowed to cure for a period of 24 h, followed by post-curing in an oven at a temperature of 120 °C for an additional 5 h.

The CFRP composite-based orthopedic implants are employed to assess the influence of AWSI machining parameters on the MRR, SR, and kerf width under both free air and underwater cutting conditions. The CFRP composite workpiece is cut into the required size, and the AWSI machining process employed is optimized for finding the influence of process parameters through Taguchi design. Taguchi designs, chosen based on the number of input factors and their levels, are validated for the entire experimentation, ensuring a minimal number of experiments while yielding acceptable results. The selection of a specific parameter for further optimization hinges on the total degree of freedom (DOF), which is calculated from the main effects of all factors involved in the experiment. Tables 1 and 2 outline the total DOF for the factors considered in the present study for free air cutting and underwater cutting. The chosen process parameters for AWSI machining include abrasive size, SOD, abrasive concentration, and feed. For abrasive size, the study considers 100 grit, 120 grit, and 140 grit, selected based on the minimum and maximum materials removed by abrasive particles. SOD is set at 1, 3, and 5 mm to account for the observed minimum and maximum MRRs. The abrasive concentration is varied at 100, 150, and 200 g, while the feed of abrasive particles is adjusted to 30, 45, and 60 mm/min. A total of nine experimental trials are conducted, determined through an initial dry run that establishes the minimum and maximum ranges for the process parameters. This approach, incorporating intermittent parameters, proves sufficient for deterministically identifying the comprehensive variable and compiling the outcomes.

2.1 AWSJ machining parameters

The parameters associated with AWSJ machining can be categorized into process parameters and performance

Table 1: AWSJ machining parameters and their levels

SI. no.	Parameter	Levels		
		Level-1	Level-2	Level-3
1	Abr. size (grit)	#100	#120	#140
2	SOD (mm)	1	3	5
3	Abr. con. (g)	100	150	200
4	Feed (mm/min)	30	45	60

Table 2: Factor settings and response parameters for free air cutting

Expt. no.	Abr. size (grit)	SOD (mm)	Abr. con. (g)	Feed (mm/min)	MRR (g/min)	TKW (mm)	BKW (mm)	SR (µ)
1	#100	1	100	30	1.79	1.84	0.93	8.93
2	#100	3	150	45	2.02	1.76	0.91	9.06
3	#100	5	200	60	2.44	2.01	0.89	9.25
4	#120	1	150	60	1.56	1.52	0.82	9.59
5	#120	3	200	30	2.15	1.98	0.97	8.54
6	#120	5	100	45	2.09	2.10	0.98	9.10
7	#140	1	200	30	1.60	1.35	0.87	9.21
8	#140	3	100	60	1.56	1.14	0.77	9.42
9	#140	5	150	45	2.09	2.04	0.96	8.65

parameters. The cutting process is influenced by three distinct groups of process parameters, namely, abrasive suspension parameters, nozzle characteristics, and system operational parameters [1,3]. The specific parameters used for the AWSI machining of CFRP composite-based orthopedic implants in the present work are given in Table 1.

Upon closely scrutinizing Table 1, it becomes evident that a thorough understanding of the distinct process parameters is crucial for a deterministic modeling of the process. This realization prompted the establishment of precise conditions for conducting pilot experiments. The experimental trials were meticulously executed for free air and underwater suspension jet machining under standard atmospheric conditions, wherein the ambient pressure of air was diligently accounted for at 101.325 kPa. Additionally, the density of air was considered at 1.225 kg/m³, and the temperature of the setup was carefully maintained at 288.15 K. These controlled parameters lay the foundation for robust and replicable experimental procedures, ensuring a comprehensive exploration of the underlying processes. The selection of process parameters is a critical aspect in AWSI machining of composites. The work of El-Hofy M has been referred to understand the criticality of selection of process parameters for machining multilayered composites [26].

2.2 Taguchi method

The Taguchi method proves to be a potent statistical tool applied in optimizing engineering and manufacturing processes [26,27], as demonstrated in the research concerning AWSJ machining for CFRP composite-based orthopedic implants. In this study, the Taguchi method was instrumental in examining the influence of critical process parameters - speed, feed, and SOD - on the kerf width and SR under free air and underwater cutting conditions [28]. The research findings unequivocally favored underwater cutting, revealing its superiority over free air cutting in achieving desirable machining outcomes. Notably, an expansion of the jet diameter in free air cutting led to a reduction in the kerf width and SR, while underwater cutting exhibited improvements in both parameters with an expanded jet diameter. Moreover, underwater cutting demonstrated reduced nozzle vibration during high-pressure operations, resulting in decreased kerf width and improved SR, emphasizing its advantages for precise and refined machining outcomes [29,30]. Utilizing the Taguchi method allowed for the systematic optimization of process parameters, enabling the identification of optimal settings for speed, feed, and SOD. This systematic approach facilitated the determination of influential factors and their optimal levels for attaining superior machining results in CFRP composite materials across both cutting conditions. The Taguchi method encompasses several equations and concepts to optimize the quality of products and processes [31,32]. One of the fundamental equations associated with the Taguchi method is the signalto-noise (S/N) ratio. The S/N ratio in Equation (1) is used to evaluate the quality characteristics of a product or process by considering the mean and variance of the responses.

The general form of S/N ratio equation from Ramesha et al. [3] is given as follows:

$$S/N = -10 \times \log_{10} \left(\frac{1}{n} \sum_{i=1}^{n} \left(\frac{Y_i}{\sigma^2} \right) \right), \tag{1}$$

where n is the number of experimental runs, Y_I is the response value for ith experimental run, and σ^2 is the variance.

2.3 **RSM**

RSM represents a statistical approach utilized for modeling and analyzing the intricate relationship between various process variables and the desired response in engineering and manufacturing contexts [33]. In the specific domain of AWSJ machining applied to CFRP composite-based

orthopedic implants, RSM serves as a valuable tool for optimizing machining parameters and predicting the machining performance. RSM entails fitting a mathematical model, often in the form of a polynomial equation, to experimental data obtained from designed experiments where process variables like jet speed, feed rate, and SOD are systematically varied. The ultimate objective lies in determining the optimal combination of these variables that results in the desired machining response, such as minimizing the SR or kerf width. By analyzing the regression model derived from experimental data, researchers can discern the significance of each process variable and uncover potential interactions between them, paving the way for informed decision-making in process optimization. With validated regression models, RSM enables the prediction of machining outcomes for different sets of process variables within the experimental domain, facilitating the identification of optimal process settings to enhance machining precision and efficiency in CFRP composite-based orthopedic implant machining applications [34]. RSM involves fitting a mathematical model to experimental data to represent the relationship between the response variable and the process variables. The general form of the polynomial equation used in RSM is given by Equation (2) [33].

$$Y = f(X_1, X_2, ..., X_p) + \varepsilon,$$
 (2)

where Y is the response variable, X_1 , X_2 , ..., X_P are the independent variables, and f is the response surface function representing the relationship between the independent variables and the response.

3 Results and discussion

The results and discussion for the machining process accomplished and statistical validations carried out are presented in this section under two subheadings, *viz.* free air and underwater suspension jet machining conditions, with critical inferences drawn for each of the two conditions of AWSJ machining considered for the present work.

3.1 Free air cutting conditions

Table 2 depicts the data from experiments investigating the effects of varying factor settings on response parameters in AWSJ machining conducted in a free air cutting environment. These experiments explore different combinations of abrasive size, SOD, abrasive concentration, and feed

rate to analyze their impact on the MRR, top and bottom kerf widths, and SR. By altering these factors, the changes in grit size, SOD, concentration, and feed rate influence the efficiency of material removal, the width of the cut at the top and bottom surfaces, and the smoothness of the machined surface can be critically observed. The data serve as a basis for identifying optimal machining conditions that result in higher MRRs, precise kerf widths, and smoother surface finishes, which are crucial for enhancing the performance and quality of AWSJ machining processes in various industrial applications.

The recorded response data in the table are critically analyzed, and the MRR, which is an important response for effectively understanding the machining process, is subjected to Taguchi analysis to determine the significant factors at 95% confidence level. The results of Taguchi's optimization, specifically for MRR in free air cutting are outlined in Tables 3–5. By examining the *F*-value in the analysis of variance (ANOVA), Table 5, one can discern the impact of various process parameters on MRR during free air cutting.

A factor is deemed significant if alterations in its value result in a significant change in the response value. This implies that variations in the response value primarily stem from intentional adjustments to the process parameter value rather than random chance. The average value of the responses at each level of an individual factor is referred to as the main effects of process parameters on MRR under free air cutting conditions.

Table 3: Response table for S/N ratios (larger is better)

Level	Abrasive size (grit)	SOD (mm)	Abr. con. (g)	Feed (mm/min)
1	3.152	2.167	2.554	2.631
2	2.819	2.770	2.729	3.152
3	2.391	3.426	3.080	2.579
Delta	0.761	1.259	0.526	0.573
Rank	2	1	4	3

Table 4: Response table for means

Level	Abrasive size (grit)	SOD (mm)	Abr. con. (g)	Feed (mm/min)
1	1.440	1.284	1.344	1.356
2	1.387	1.379	1.372	1.438
3	1.320	1.484	1.431	1.353
Delta	0.121	0.201	0.087	0.084
Rank	2	1	3	4

Table 5: ANOVA of MRR in free air cutting conditions

Source	Sum of squares	DF	Mean square	<i>F</i> -value	<i>p</i> -value	Remarks
Model	0.7580	4	0.1895	65.79	0.0007	Significant
A – Abrasive size	0.1667	1	0.1667	57.86	0.0016	
B – SOD	0.4940	1	0.4940	171.51	0.0002	
C – Abrasive concentration	0.0725	1	0.0725	25.19	0.0074	
D – Feed	0.0328	1	0.0328	11.39	0.0279	
Residual	0.0115	4	0.0029			
Cor total	0.7696	8				

3.1.1 Results of the Taguchi method for MRR for free air cutting

Figure 2 shows the main effects plot for means for MRR. It is evident that the abrasive size of 100 grit (level 1), SOD of 5 mm (level 3), abrasive concentration of 200 g (level 3), and feed rate of 45 mm/min (level 2) give the mean for each combination of control factor levels in the design for optimizing the MRR as per the Taguchi's condition of larger is better.

From, the main effects plot for S/N ratios seen for MRR in Figure 3, it is evidenced that the optimized set of process parameters, *viz.* abrasive size of 100 grit, SOD of 5 mm, abrasive concentration of 200 g, and feed rate of 45 mm/min give the maximum MRR.

The response table for S/N ratios is given in Table 3. It is seen from the table that the SOD has a significant effect on MRR, followed by the abrasive size, feed, and abrasive concentration.

The response table for means for MRR is given in Table 4. It is seen from the table that the SOD has a significant effect on the mean for each combination of control factor levels in the design for optimizing the MRR, followed by the abrasive size, abrasive concentration, and feed rate.

3.1.2 Results of RSM for MRR for free air cutting

The RSM accomplished for MRR for free air cutting gives the ANOVA table, surface and contour plots, and predicted *vs* actual plots for different conditions. The results of ANOVA are presented in Table 5.

The model *F*-value of 65.79 implies the model is significant. There is only a 0.07% chance that an *F*-value this large could occur due to noise.

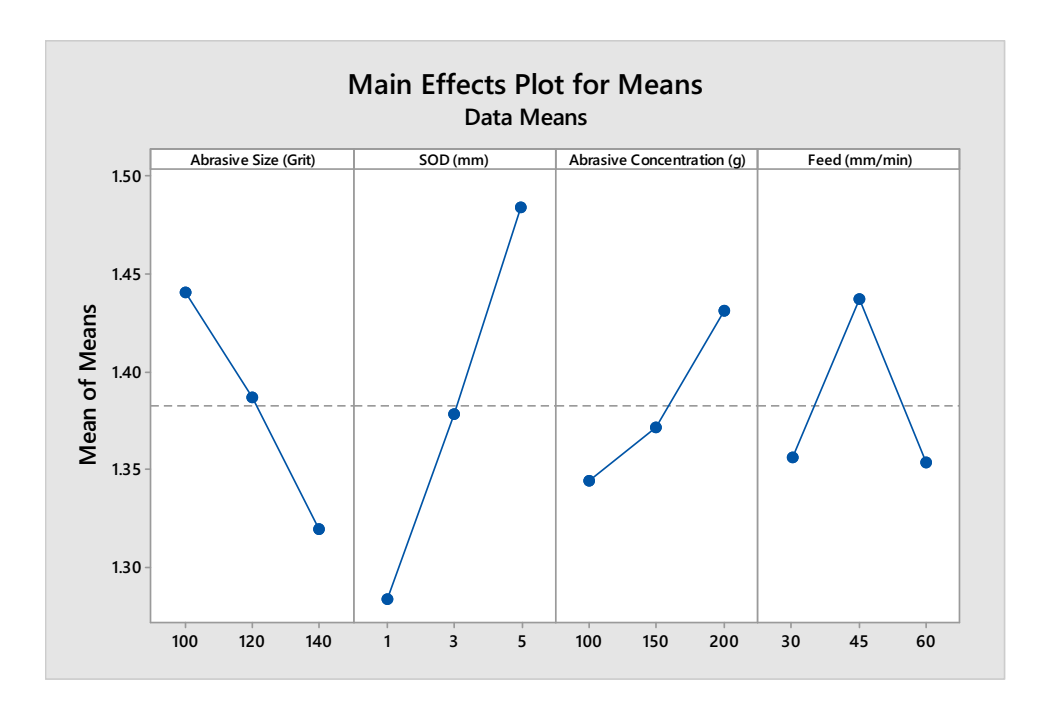


Figure 2: Main effects plot for means for MRR for free air cutting.

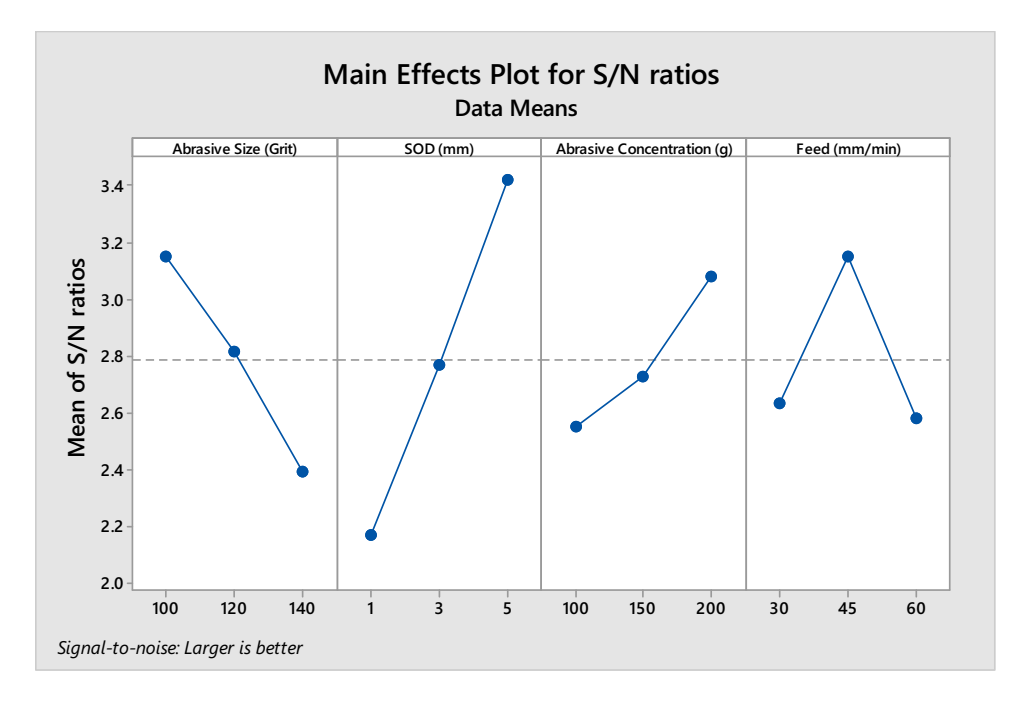


Figure 3: Mean of S/N ratios for MRR for free air cutting.

P-values less than 0.0500 indicate model terms are significant. In this case A, B, C, and D are significant model terms. Values greater than 0.1000 indicate the model terms are not significant. If there are many insignificant model terms (not counting those required to support hierarchy), model reduction may improve your model.

Figures 4 and 5 show the contour plot and surface plot illustrating the relationship between SOD and abrasive size in relation to MRR, respectively. The plots distinctly indicate that a substantial increase in abrasive particle size and SOD result in a significant boost in MRR. A larger grain size contributes to a heightened area of erosion, consequently leading to an increase in MRR. Moreover, an elevated SOD leads to a broader coverage area by the jet, thereby further enhancing the MRR.

Figures 6 and 7 display the contour plot and surface plot, illustrating the correlation between SOD and abrasive concentration in relation to MRR, respectively. The plots

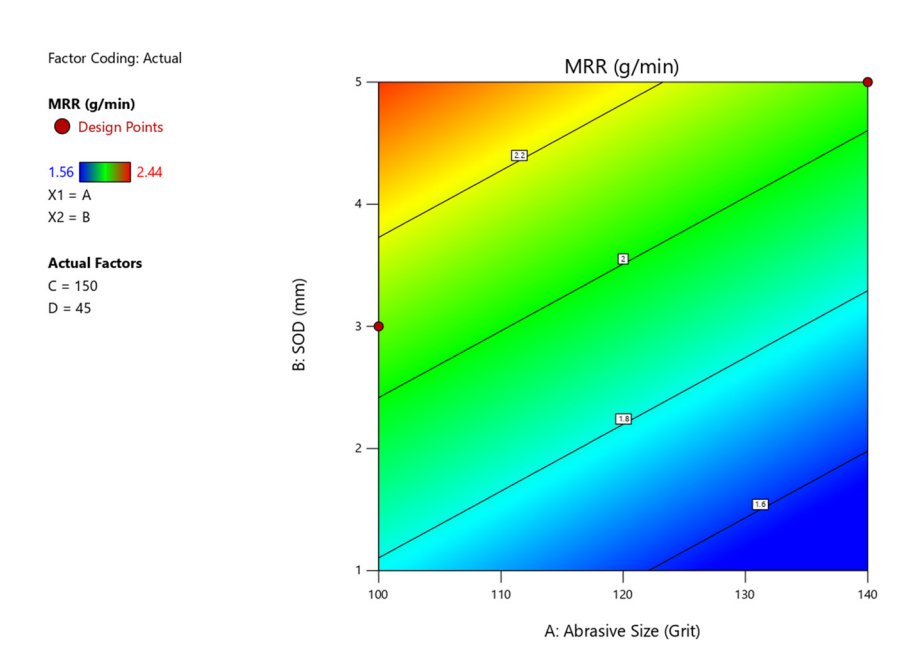


Figure 4: Contour plot of SOD vs abrasive size for MRR for free air cutting.

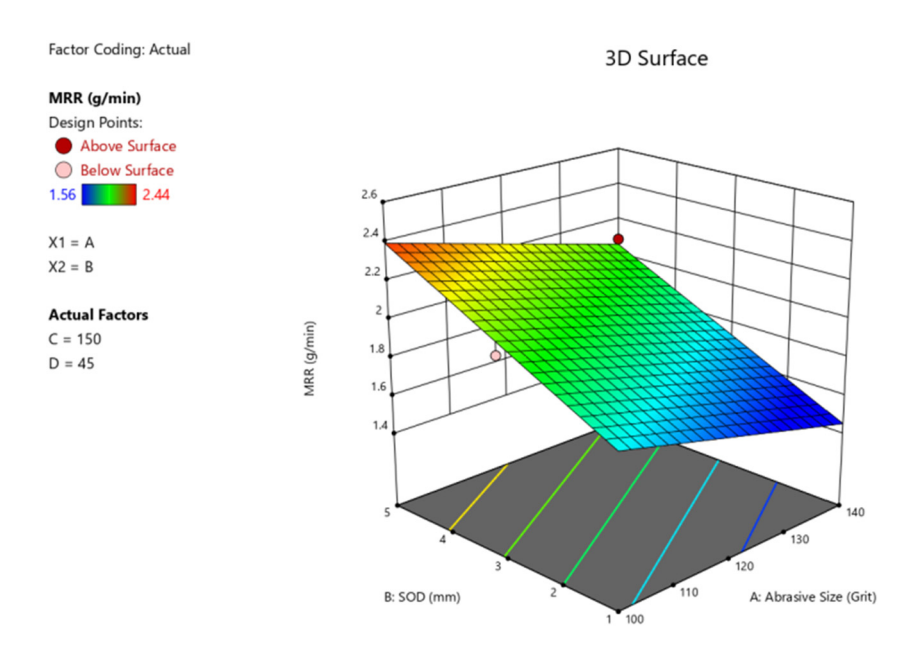


Figure 5: 3D surface plot of SOD vs abrasive size for MRR for free air cutting.

distinctly reveal that a noteworthy escalation in SOD and abrasive concentration correlates with a significant upsurge in MRR. An increase in abrasive concentration intensifies the frequency of particles participating in the erosion process, consequently leading to an augmentation in MRR. Additionally, a heightened SOD contributes to a more extensive coverage area by the jet, further amplifying the MRR. The combined impact of both parameters results in a higher MRR.

Figures 8 and 9 present the contour plot and surface plot illustrating the correlation between the SOD and feed rate in relation to MRR, respectively. The plots distinctly reveal that a noteworthy increase in SOD, coupled with a decrease in the feed rate, results in a significant enhancement of MRR. An escalation in the feed rate contributes to a reduction in MRR due to a decrease in abrasive flow velocity. Consequently, the limited kinetic energy of the jet gets distributed over a larger number of particles, resulting in a

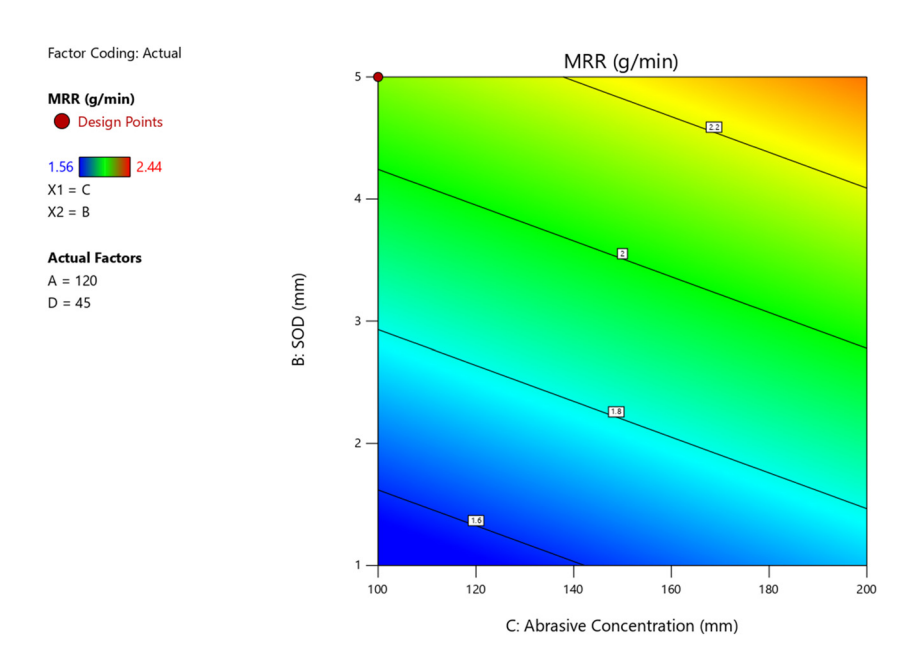


Figure 6: Contour plot of abrasive concentration vs SOD for MRR for free air cutting.

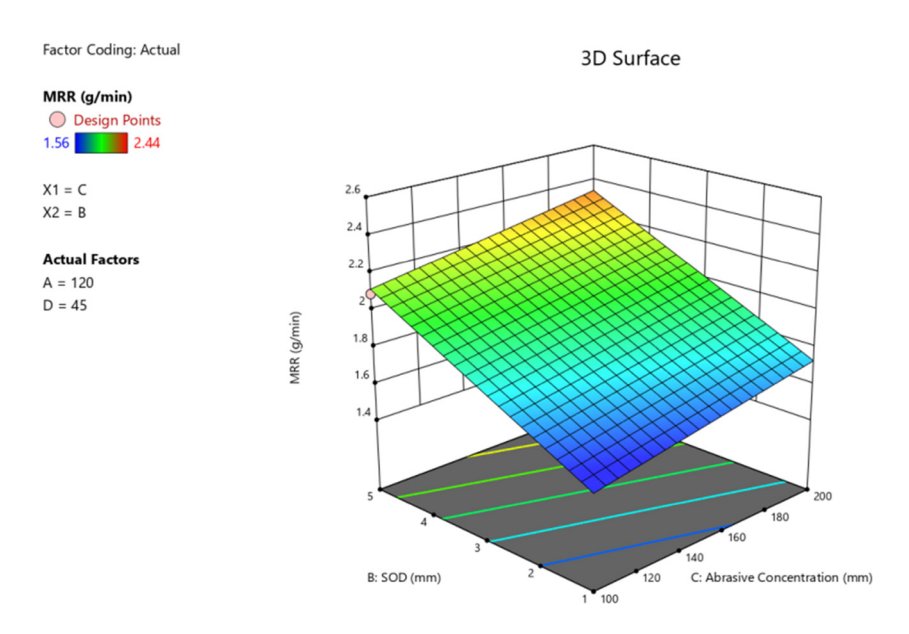


Figure 7: 3D surface plot of abrasive concentration vs SOD for MRR for free air cutting.

diminished kinetic energy for each specific particle. This phenomenon also leads to an increase in turbulence. Furthermore, an elevated SOD amplifies the coverage area by the jet, further augmenting the MRR. The combined impact of both parameters yields a higher MRR. Figure 10 gives the predicted *vs* actual plot of MRR for free air cutting for different sets of AWSI machining conditions.

Table 6 gives the fit statistics of RSM for MRR for free air machining conditions. The predicted R^2 of 0.9184 is in

reasonable agreement with the adjusted R^2 of 0.9701, *i.e.*, the difference is less than 0.2. The Adeq Precision measures the S/N ratio. A ratio greater than 4 is desirable. The ratio of 22.203 indicates an adequate signal. This regression fit statistics can be effectively employed to evolve newer design spaces.

Equation (3) gives the regression equation obtained from the RSM analysis of the parameters on MRR, which can be effectively used to predict the outcomes for different input conditions.

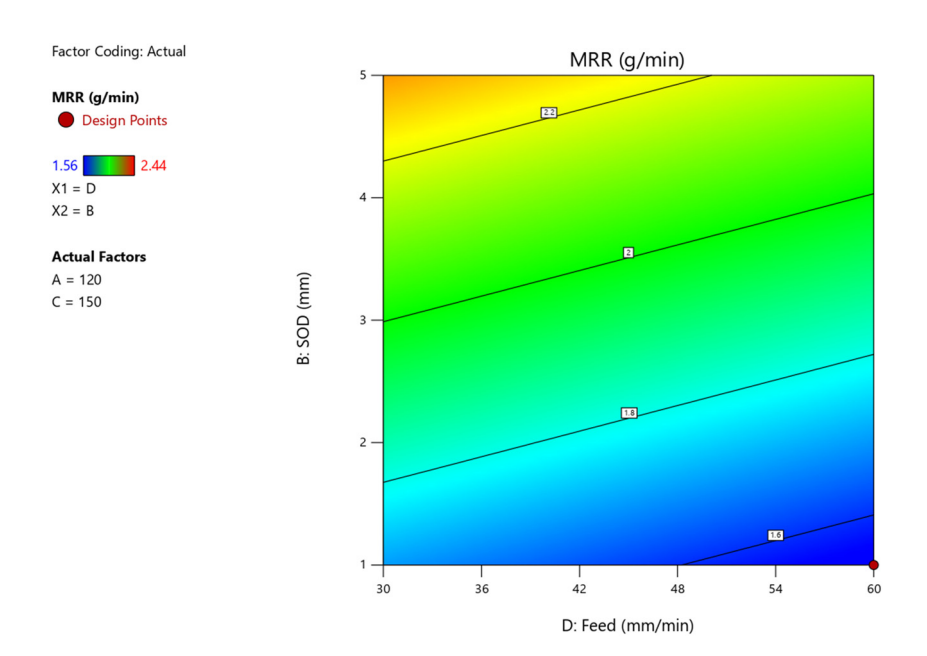


Figure 8: Contour plot of feed vs SOD for MRR for free air cutting.

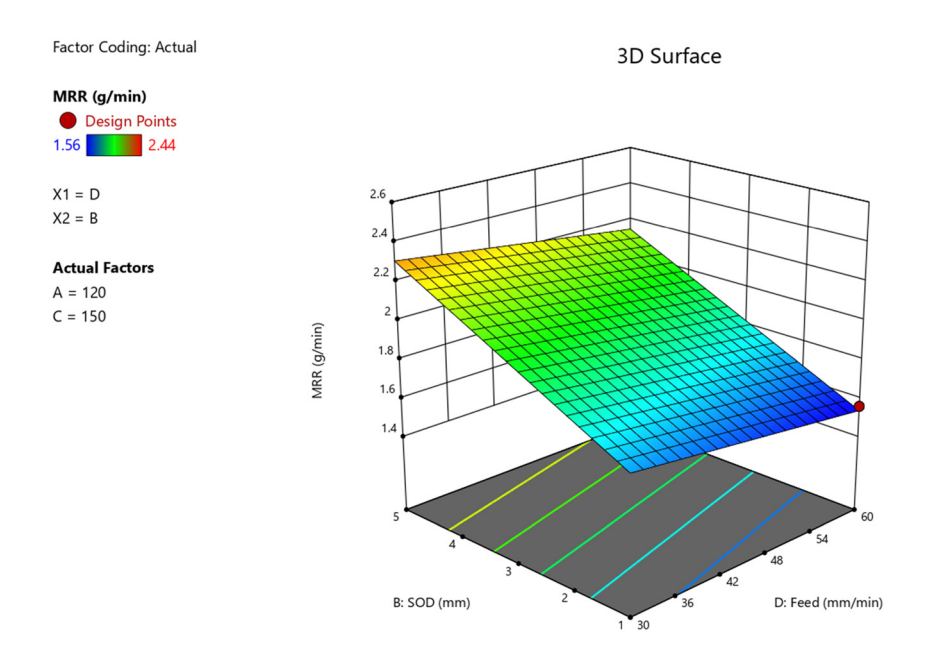


Figure 9: 3D surface plot of feed vs SOD for MRR for free air cutting.

The results of present work are compared with the findings of Santhosh *et al.* [29,30] who have successfully conducted several studies on optimizations through the application of RSM. This involved a detailed analysis of experimental trials and

their outcomes, focusing on critical aspects and validations. Their efforts were directed toward optimizing experimental parameters for wear in composites. The reported results indicate that the chosen optimum parameters not only enhance the wear resistance but also reduce the wear resistance by 22%. Similarly, in the present work, the MRR improves, while the SR reduces. This improvement is attributed to the careful selection of appropriate SOD and traverse speed during the AWSJ machining process.

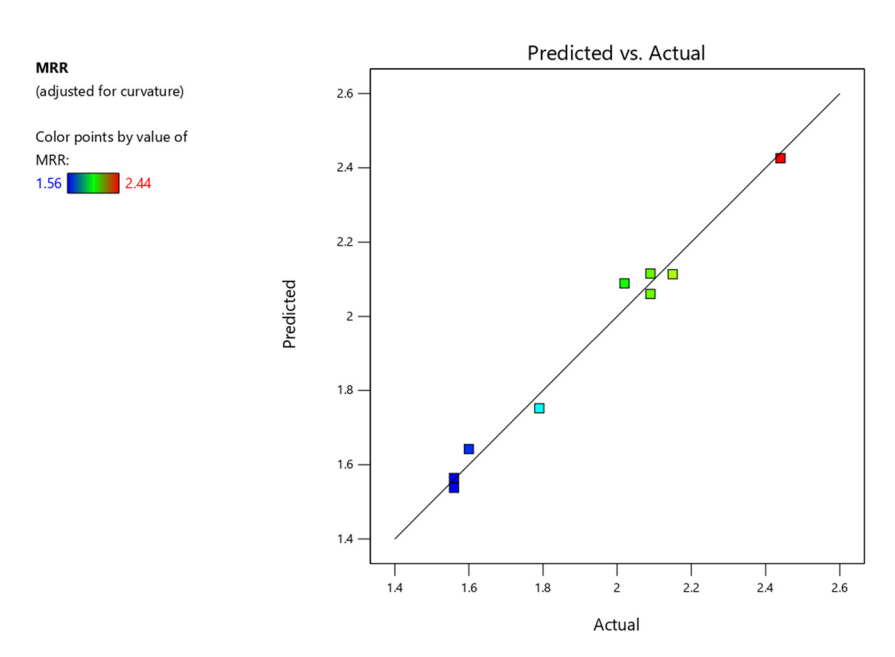


Figure 10: Predicted vs actual plot of MRR for free air cutting.

Table 6: Fit statistics of RSM for MRR for free air conditions

Std. dev.	0.0537	R^2	0.9850
Mean	1.92	Adjusted R ²	0.9701
C.V. %	2.79	Predicted R ²	0.9184
		Adeq precision	22.2027

RSM stands out as a potent instrument for fine-tuning parameters within manufacturing processes. By harnessing mathematical and statistical methodologies, RSM aids in unraveling intricate connections between input variables and desired output responses. In machining and production domains, RSM serves to amplify process efficacy, curtail expenses, and elevate product standards [31]. One key merit of RSM lies in its capacity to streamline the number of experimental trials necessary for optimization. Instead of exhaustively testing every conceivable parameter combination, RSM enables researchers to judiciously select a subset of experiments grounded in statistical design principles like factorial or fractional factorial designs. This strategy not only conserves resources but also furnishes valuable insights into the interrelations among diverse variables. Additionally, RSM facilitates the identification of optimal parameter configurations that maximize desired outcomes while minimizing variations and defects. By constructing response surfaces and contour plots, engineers can visually map the nexus between input parameters and performance metrics, thereby facilitating informed decision-making and process enhancement. RSM finds practical utility across a spectrum of manufacturing applications, encompassing composite fabrication and machining. Its adaptability and efficacy render it indispensable for industries striving to bolster productivity and maintain a competitive edge in today's dynamic market milieu [32,33]. The same holds good in the present work, wherein the MRR is considered for optimizing the process parameters in the AWSI machining process for two cutting conditions.

The results of AWSI machining of CFRP compositebased orthopedic implants in the present work are further compared with the findings of Santhana kumar et al. [34], who have applied grey-based RSM for optimizing AWSI cutting parameters in ceramic tile machining. Their study addresses the challenges of achieving precise cuts and minimizing SR in ceramic tile processing, which are critical factors in ensuring quality and efficiency in the manufacturing industry. They have conducted experimental trials to investigate the effects of key cutting parameters such as jet pressure, abrasive flow rate, SOD, and traverse speed on MRR and SR. By employing grey relational RSM techniques, they were able to model the complex relationships between process variables and performance metrics. The findings of the study provide valuable insights into the optimal parameter settings that enhance the cutting efficiency and quality in AWSI machining of ceramic tiles. In the present work, through systematic experimentation and analysis, it is herewith observed that the MRR in the AWSI machining process for composites is a critical factor, which depends on the abrasive size, concentration, nozzle SOD, and suspension of composites in water for increasing the MRR and the machining quality for the composites.

3.2 Underwater AWSJ cutting conditions

Table 7 outlines the experimental setup and results for underwater cutting, specifically examining the influence of different factor settings on various response parameters. Each experiment, labeled from 1 to 9, investigates combinations of abrasive size, SOD, abrasive concentration, and feed rate, measuring their impact on MRR, top and bottom kerf widths (TKW and BKW, respectively), and SR. By altering factors such as abrasive size, SOD, concentration, and feed rate, researchers observed changes in the efficiency of material removal, the width of the cut at different

Table 7: Factor settings and response parameters for underwater cutting

Expt. no.	Abr. size (grit)	SOD (mm)	Abr. con. (g)	Feed (mm/min)	MRR (g/min)	TKW (mm)	BKW (mm)	SR (µ)
1	#100	1	100	30	1.90	1.79	0.80	8.16
2	#100	3	150	45	2.12	1.83	0.84	8.73
3	#100	5	200	60	2.62	1.78	0.78	8.85
4	#120	1	150	60	1.65	1.56	0.71	8.96
5	#120	3	200	30	2.42	1.82	0.84	8.22
6	#120	5	100	45	2.27	1.88	0.79	8.76
7	#140	1	200	30	1.71	1.70	0.81	8.69
8	#140	3	100	60	1.65	1.54	0.67	9.1
9	#140	5	150	45	2.18	1.85	0.84	8.21

Table 8: Response table for S/N ratios (larger is better)

Level	Abrasive size (grit)	SOD (mm)	Abr. con. (g)	Feed (mm/min)
1	6.304	4.334	5.107	5.263
2	5.638	5.539	5.457	6.304
3	4.783	6.851	6.160	5.158
Delta	1.521	2.517	1.052	1.147
Rank	2	1	4	3

depths, and the smoothness of the machined surface. The data provide insights into optimal conditions for underwater cutting processes, aiming for higher MRRs, precise kerf widths, and improved surface finishes, crucial for enhancing the effectiveness and quality of underwater cutting applications across various industries.

The recorded response data in this table, including MRR, TKW, BKW, and SR, were subject to ANOVA to determine the significant factors at a 95% confidence level. The ANOVA results, specifically for MRR in underwater cutting, are outlined in Table 10. By examining the *F*-value in these tables, one can discern the impact of various process parameters on MRR during free air cutting.

3.2.1 Results of the Taguchi method for MRR for underwater cutting

The provided response in Table 8 illustrates the S/N ratios (larger is better) for different levels of abrasive size (grit), SOD (mm), abrasive concentration (g), and feed rate (mm/min) in the context of underwater AWSJ machining. The table displays S/N values corresponding to each level of factors, with higher values indicating a better performance. Additionally, the "Delta" row showcases the differences between the highest and the lowest S/N values within each factor, while the "Rank" row assigns a rank to each factor based on their S/N values, with lower ranks signifying better performance. This analysis aids in identifying the most

Table 9: Response table for means

Level	Abrasive size (grit)	SOD (mm)	Abr. con. (g)	Feed (mm/min)
1	2.083	1.650	1.813	1.847
2	1.933	1.910	1.890	2.067
3	1.750	2.207	2.063	1.853
Delta	0.333	0.557	0.250	0.220
Rank	2	1	3	4

influential factors and optimal levels for achieving improved outcomes in underwater AWSJ machining processes. It is seen from the table that the SOD has a significant effect on MRR, followed by the abrasive size, feed, and abrasive concentration.

The response table for means for MRR is given in Table 9. It is seen from the table that the SOD has a significant effect on the mean for each combination of control factor levels in the design for optimizing the MRR, followed by abrasive size, abrasive concentration, and feed rate. Figure 11 shows the main effects plot for means for MRR. It is evident that the abrasive size of 100 grit (level 1), SOD of 5 mm (level 3), abrasive concentration of 200 g (level 3), and feed rate of 45 mm/min (level 2) give the mean for each combination of control factor levels in the design for optimizing the MRR as per Taguchi's condition of larger is better. From the main effects plot for S/N ratios seen for MRR in Figure 12, it is evidenced that the optimized set of process parameters, *viz.* the abrasive size of 100 grit, SOD of 5 mm, abrasive concentration of 200 g, and feed rate of 45 mm/min gives the maximum MRR.

3.2.2 Results of ANOVA for MRR for underwater cutting

Table 10 gives the ANOVA of MRR in underwater cutting conditions. The model F-value of 25.47 implies the model is significant. There is only a 0.42% chance that an F-value this large could occur due to noise. From the ANOVA table, it is herewith observed that p-values <0.0500 indicate

Table 10: ANOVA of MRR in underwater cutting conditions

Source	Sum of squares	DF	Mean square	<i>F</i> -value	<i>p</i> -value	Remarks
Model	0.9522	4	0.2380	25.47	0.0042	significant
A – Abrasive size	0.2017	1	0.2017	21.58	0.0097	
B – SOD	0.6060	1	0.6060	64.84	0.0013	
C – Abrasive concentration	0.1091	1	0.1091	11.67	0.0269	
D – feed	0.0603	1	0.0603	6.46	0.0639	
Residual	0.0374	4	0.0093			
Cor total	0.9896	8				

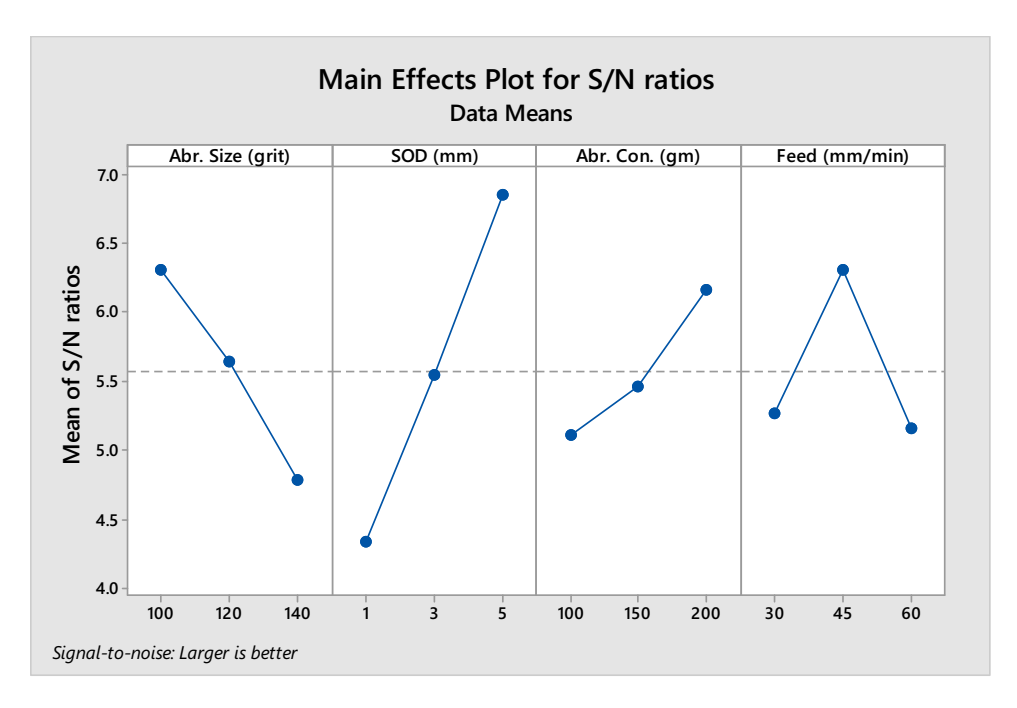


Figure 11: Main effects plot for means for MRR for underwater cutting.

model terms are significant. In this case A, B, and C are significant model terms. Values greater than 0.1000 indicate the model terms are not significant. If there are many insignificant model terms (not counting those required to support hierarchy), model reduction may improve the model.

Figures 13 and 14 show the contour plot and surface plot illustrating the relationship between SOD and abrasive size in relation to MRR, respectively. The plots distinctly indicate that a substantial increase in abrasive particle size and SOD results in a significant boost in MRR. A larger grain size contributes to a heightened area of erosion,

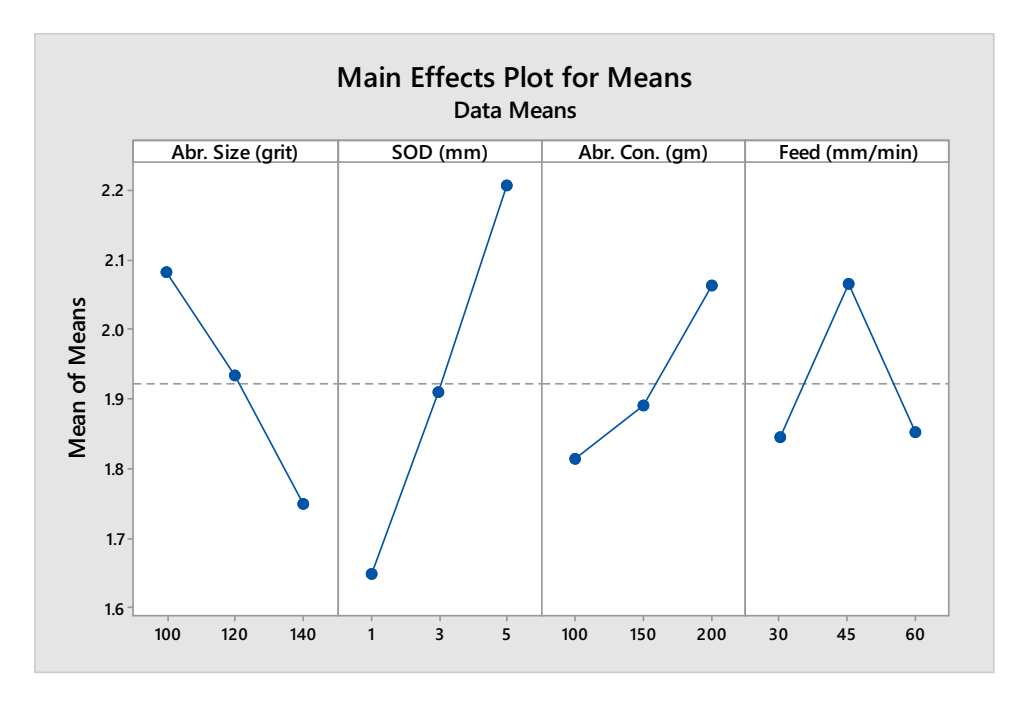


Figure 12: Mean of S/N for MRR for underwater cutting.

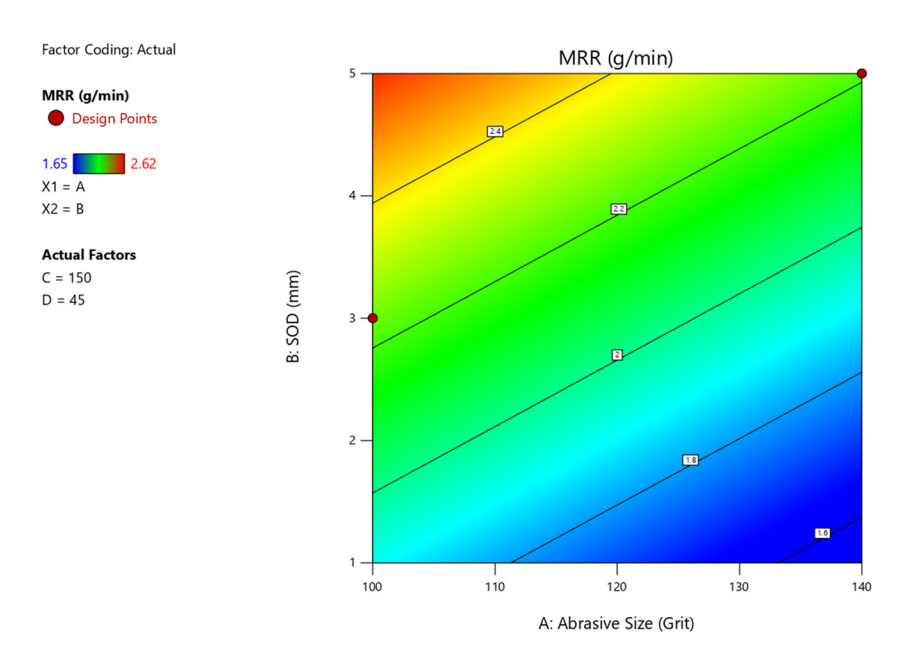


Figure 13: Contour plot of SOD vs abrasive size for MRR for underwater cutting.

consequently leading to an increase in MRR. Moreover, an elevated SOD leads to a broader coverage area by the jet, thereby further enhancing the MRR.

Figures 15 and 16 display the contour plot and surface plot, illustrating the correlation between SOD and abrasive concentration in relation to MRR, respectively. The plots distinctly reveal that a noteworthy escalation in SOD and abrasive concentration correlates with a significant upsurge in MRR. An increase in the abrasive concentration intensifies the frequency of particles participating in the erosion

process, consequently leading to an augmentation in MRR. Additionally, a heightened SOD contributes to a more extensive coverage area by the jet, further amplifying the MRR. The combined impact of both parameters results in a higher MRR.

Figures 17 and 18 present the contour plot and surface plot illustrating the correlation between the SOD and feed rate in relation to MRR, respectively. The plots distinctly reveal that a noteworthy increase in SOD, coupled with a decrease in the feed rate, results in a significant

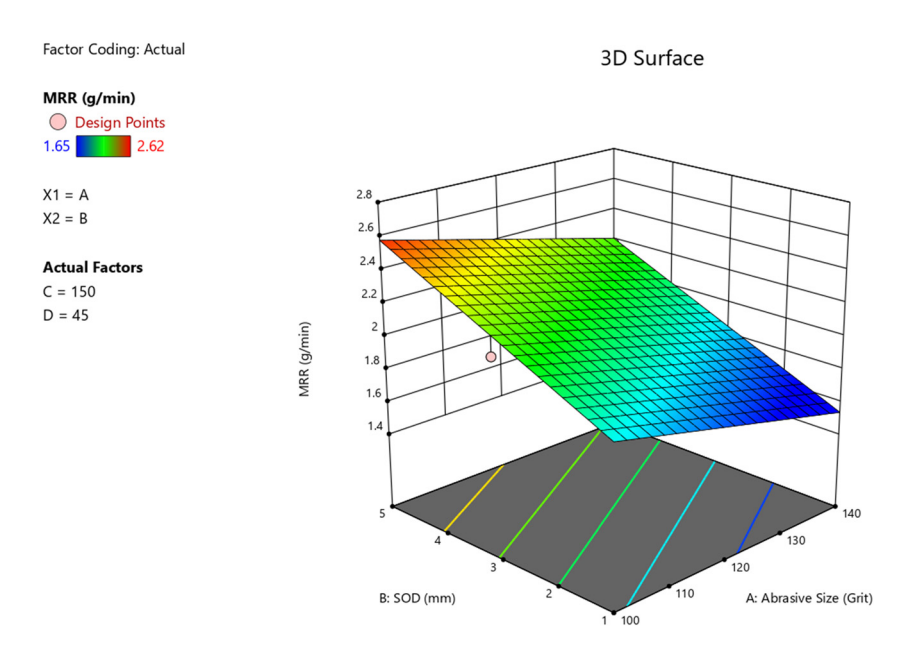


Figure 14: 3D surface plot of SOD vs abrasive size for MRR for underwater cutting.

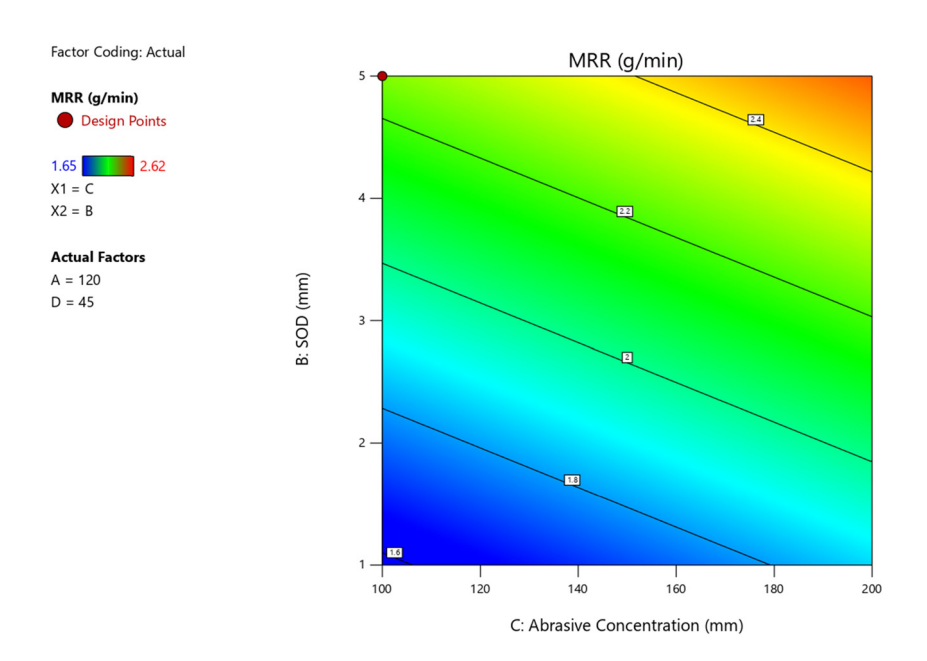


Figure 15: Contour plot of abrasive concentration vs SOD for MRR for underwater cutting.

enhancement of MRR. An escalation in feed rate contributes to a reduction in MRR due to a decrease in the abrasive flow velocity. Consequently, the limited kinetic energy of the jet gets distributed over a larger number of particles, resulting in a diminished kinetic energy for each specific particle. This phenomenon also leads to an increase in turbulence. Furthermore, an elevated SOD amplifies the coverage area by the jet, further augmenting the MRR. The combined impact of both parameters yields a higher MRR. Figure 19 gives the predicted vs actual plot for the

MRR for underwater cutting. It is herewith evident that the actual results are in close agreement with the predicted results.

Table 11 presents the fit statistics of MRR for underwater cutting. The predicted R^2 of 0.8572 is in reasonable agreement with the adjusted R^2 of 0.9244, *i.e.*, the difference is less than 0.2.

Adeq Precision measures the S/N ratio. A ratio greater than 4 is desirable. The ratio of 13.818 indicates an adequate signal. The regression equation of MRR for

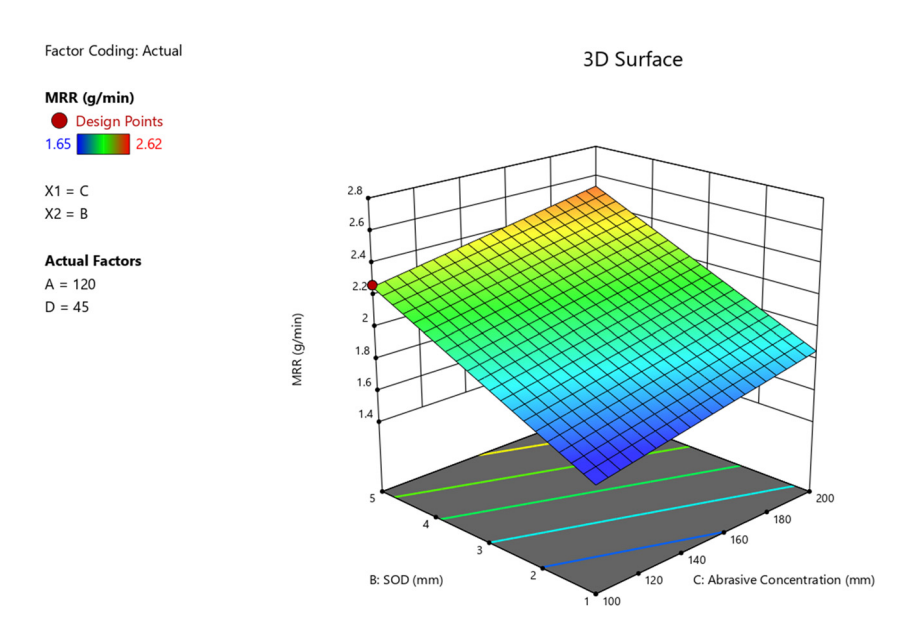


Figure 16: 3D surface plot of abrasive concentration vs SOD for MRR for underwater cutting.

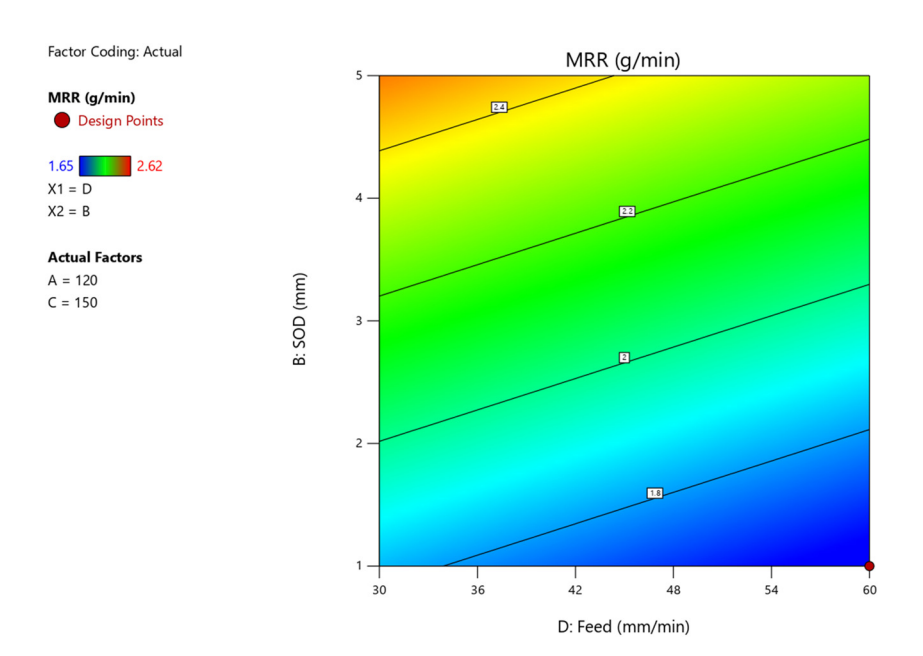


Figure 17: Contour plot of feed vs SOD for MRR for underwater cutting.

underwater cutting is given in Equation (4). The equation holds good, and it can be effectively employed to design newer arrays of experimentations.

MRR =
$$+2.56447 - 0.009167 \times \text{Abrasive Size}$$

+ $0.168844 \times \text{SOD}$
+ $0.002740 \times \text{Abrasive Concentration} -$
 $0.007204 \times \text{Feed}$. (4)

The results of the present work are compared with the findings of Alberdi *et al.* [35]; the study explores the effectiveness of AWJ in machining composite materials, aiming to understand its capabilities and limitations. Through experimentation and analysis, the authors examine various factors influencing the cutting process, including the abrasive size, SOD, feed rate, and cutting speed. Their work provides insights into the mechanisms involved in

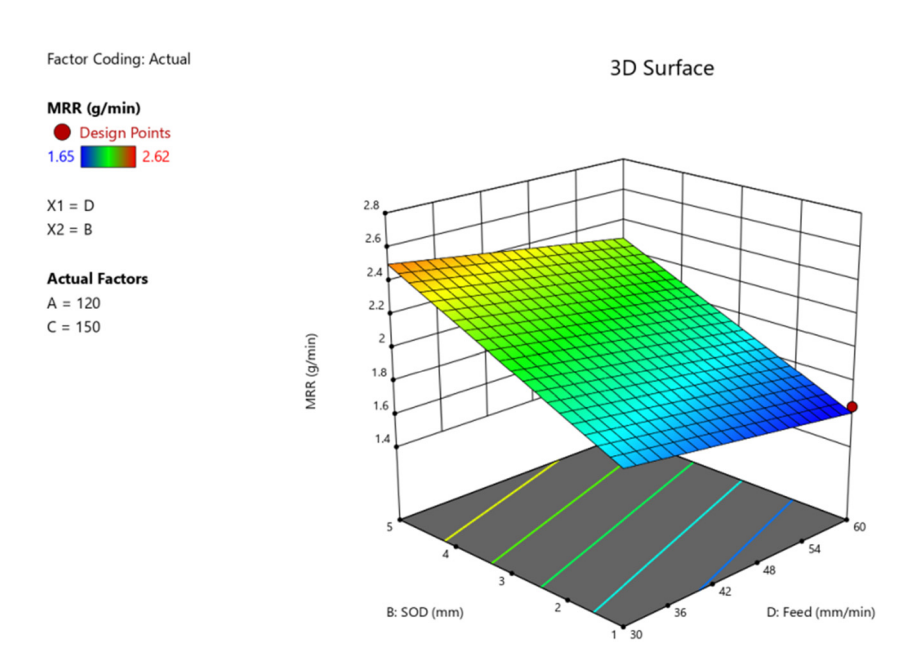


Figure 18: 3D surface plot of feed vs SOD for MRR for underwater cutting.

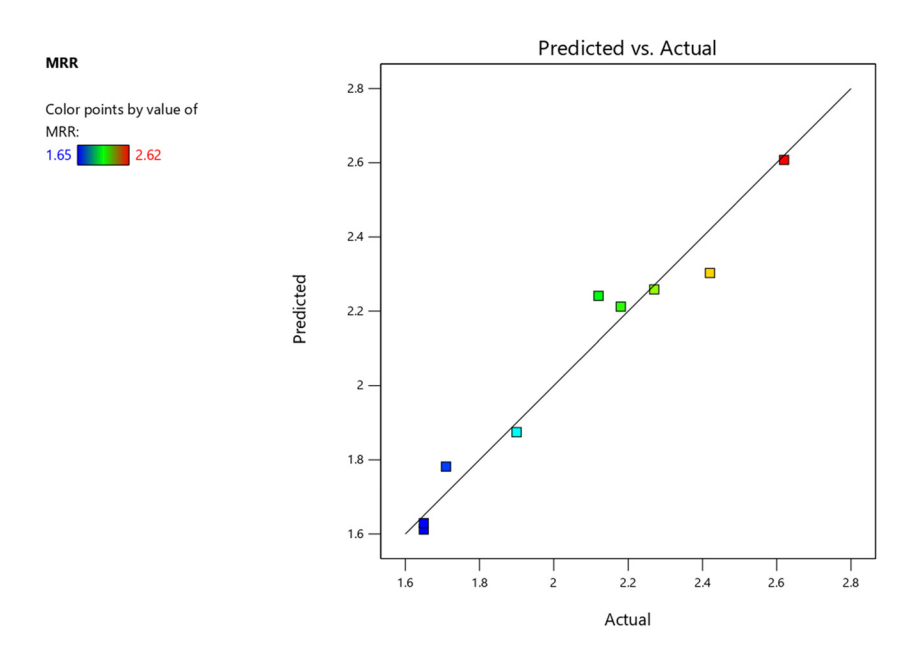


Figure 19: Predicted vs actual plot of MRR for underwater cutting.

composite cutting with AWJ only; however, the present work has explored the AWSJ process in both free air and underwater conditions and has additionally explored challenges and opportunities for further research in this field, contributing to the advancement of composite machining techniques.

The work of Alberdi et al. also delves into the effect of energy consumption and temperature of the abrasive water in the composite cutting process. It explores how variations in energy consumption and temperature can impact the efficiency and effectiveness of the cutting operation. By analyzing these factors, the authors aim to optimize the cutting process to minimize energy consumption while maintaining desired cutting performance. Additionally, the article discusses the thermal effects of abrasive water on the workpiece material and how temperature changes can affect the material properties and cutting quality. Variations in temperature influence the viscosity and density of the abrasive-water mixture, affecting the cutting efficiency, while thermal effects on the workpiece material can lead to dimensional inaccuracies and structural damage. Overall, the investigation into energy consumption and temperature

Table 11: Fit statistics of MRR for underwater cutting

Std. dev.	0.0967	R^2	0.9622
Mean	2.06	Adjusted R ²	0.9244
C.V. %	4.70	Predicted R ²	0.8572
		Adeq precision	13.8178

provides valuable insights into improving the sustainability and precision of AWI cutting for composite materials [35].

4 Conclusions

The conclusions drawn from the analysis of AWSJ machining on CFRP composite-based orthopedic implants provide valuable insights based on numerical findings and statistical validations.

- SOD emerges as the most influential factor in controlling MRR, with underwater cutting consistently outperforming free air cutting.
- For instance, at #100 abrasive size and 5 mm SOD, the MRR peaked at 2.44 g/min, while an increase in abrasive size correlated with higher MRR values, such as achieving 2.15 g/min at #120 grit and 3 mm SOD.
- Furthermore, the study highlights the significance of traverse rate and SOD in controlling the kerf width (TKW and BKW) and SR.
- Underwater cutting conditions consistently yield superior results compared to free air cutting, as evidenced by numerical values such as a kerf width of 0.89 mm and an SR of 9.25 μ m achieved under specific conditions.
- These findings underscore the effectiveness of underwater cutting and provide valuable guidance for optimizing AWSJ machining parameters for CFRP composites-based orthopedic implants.
- The Taguchi method and RSM helped in the statistical validation and optimization of the grit size, SOD, abrasive concentrations, and feed rate in underwater cutting conditions.

Acknowledgements: The authors gratefully thank their respective institutions for their strong support in this study.

Funding information: Authors state no funding involved.

Author contributions: All authors have accepted responsibility for the entire content of this manuscript and consented to its submission to the journal, reviewed all the results and approved the final version of the manuscript. RK, SN, MMC, MK, GSP and MIA: conceptualization, data curation, formal analysis, funding acquisition, investigation, methodology, project administration, resources, software, supervision, validation, visualization, writing – original draft, and writing – review and editing.

Conflict of interest: Authors state no conflict of interest.

Data availability statement: The necessary data used in the manuscript are already present in the manuscript.

References

- [1] Goto K, Imai K, Arai M, Ishikawa T. Shear and tensile joint strengths of carbon fiber-reinforced thermoplastics using ultrasonic welding. Compos Part A Appl Sci Manuf. 2019;116:126–37. doi: 10.1016/j. compositesa.2018.10.032.
- [2] Raj A, Ramesha K, Sajan JU, Khan DM, Varshini UA. Comparison of various types of lubrication during hard turning of H13 tool steel by analysing Flank wear using ANOVA. In: Vijayaraghavan L, Reddy K, Jameel Basha S, editors. Emerging trends in mechanical engineering. Lecture notes in mechanical engineering. Singapore: Springer; 2020. p. 489–97. doi: 10.1007/978-981-32-9931-3 47.
- [3] Ramesha K, Santhosh N, Kiran K, Manjunath N, Naresh H. Effect of the process parameters on machining of GFRP composites for different conditions of abrasive water suspension jet machining. Arab J Sci Eng. 2019;44:7933–43. doi: 10.1007/s13369-019-03973-w.
- [4] Pahuja R, Ramulu M. Abrasive water jet machining of Titanium (Ti6Al4V)–CFRP stacks – A semi-analytical modeling approach in the prediction of kerf geometry. J Manuf Process. 2019;39:327–37. doi: 10.1016/j.jmapro.2019.01.041.
- [5] Pahuja R, Ramulu M, Hashish M. Abrasive Water jet machining (AWJ) of hybrid Titanium/Graphite composite laminate: Preliminary results. In Proceedings of the 22nd International Conference on Water Jetting, Haarlem, the Netherlands; 3–5 September 2014. p. 83–95. doi: 10.13140/2.1.4554.1765.
- [6] Pahuja R, Ramulu M, Hashish M. Abrasive water jet profile cutting of thick Titanium/Graphitefibermetal laminate. In ASME International Mechanical Engineering Congress and Exposition. New York, NY, USA: American Society of Mechanical Engineers; 2016. p. 1–11. doi: 10.1115/IMECE2016-67136.
- [7] Li M, Huang M, Chen Y, Gong P, Yang X. Effects of processing parameters on kerf characteristics and surface integrity following abrasive water jet slotting of Ti6Al4V/CFRP stacks. J Manuf Process. 2019;42:82–95. doi: 10.1016/j.jmapro.2019.04.024.

- [8] Ramulu M, Kunapurn S, Arola D, Hashish M. Water jet machining and peening of metals. Trans ASME J Press Vessel Technol. 2000;122:90–5. doi: 10.1115/1.556155.
- [9] Wang J. The effects of the jet impact angle on the cutting performance in AWJ machining of alumina ceramics. Key Eng Mater. 2003;238–239:117–24. doi: 10.1115/1.556155.
- [10] Chen Fl. The effect of cutting jet variation on striation formation in abrasive water jet cutting. Int J Mach Tools Manuf. 2001;41(10):1479–86. doi: 10.1016/S0890-6955(01)00013-X.
- [11] Akkurt A, Kulekci MK. Effect of feed rate on surface roughness in abrasive water jet cutting applications. J Mater Process Technol. 2004;147:389–96. doi: 10.1016/j.jmatprotec.2004.01.013.
- [12] Azmir MA, Ahsan AK. A study of abrasive water jet machining process on glass/epoxy composite laminate. J Mater Process Technol. 2009;209(20):6168–73. doi: 10.1016/j.jmatprotec.2009.08.011.
- [13] Nair A, Kumanan S. Optimization of size and form characteristics using multi-objective grey analysis in abrasive water jet drilling of Inconel 617. J Braz Soc Mech Sci Eng. 2018;40:121. doi: 10.1007/ s40430-018-1042-7.
- [14] Ravi Kumar K, SreeBalaji VS, Pridhar T. Characterization and optimization of abrasive water jet machining parameters of aluminium/tungsten carbide composites. Measurement. 2018;117:57–66. doi: 10.1016/j.measurement.2017.11.059.
- [15] Deepak D, Anjaiah D, Yagnesh Sharma N. The effect of diameter ratio and abrasive grain size on exit velocity by numerical simulation of flow through abrasive water suspension jet nozzle using statistical experimental design. In 2011 WJTA-IMCA Conference and Expo, George R. Brown Convention Center, Houston, Texas, USA, 19th September – 21st September; 2011.
- [16] Anjaiah D, Chincholkar AM. Cutting of glass using low pressure abrasive water suspension jet with the addition of Zycoprint polymer. In Proceedings of 19th International Conference on Water letting, BHR Group, UK; 2008, p. 105–19.
- [17] Brandt S, Louis H, Milchers W, Mohamed M, Pude F, von Rad C. Abrasive water jets—a flexible tool for nonconventional machining. In Proceedings of 19th AIMTDR Conference, Narosa Publishing House, New Delhi, India; 2000. p. 129–34.
- [18] Santhosh N, Kempaiah UN, Manjunath N, Ramesha K. Fabrication and characterization of hybrid aluminium AA 5083/SiCP/Fly ash composites. Tathapi. 2020;19(56):236–46.
- [19] Ramesha K, Pd S, Santhosh N, Jangam S. Design and optimization of the process parameters for friction stir welding of dissimilar aluminium alloys. Eng Appl Sci Res. 2021;48(3):257–67, https:// ph01.tci-thaijo.org/index.php/easr/article/view/241021.
- [20] Ramesha K, Santhosh N, Bedi R, Sudersanan PD. A comprehensive review of novelty of friction stir welding of aluminium-magnesium alloys for advanced engineering applications. J Thin Films Coat Sci Technol Appl. 2018;5(2):7–14. https://engineeringjournals. stmjournals.in/index.php/JoTCSTA/article/view/698.
- [21] Santhosh N, Ramesha K. Mechanical and thermal characterization of friction stir weld joints of Al-Mg Alloy. Int J Res Aeronaut Mech Eng. 2017;(Special):443–53.
- [22] Hussein MA, Shamkhi HA, Abd ZN, Abbas FH. Experimental study of chemical oxygen demand removal by electrochemical oxidation treatment of petroleum refinery wastewater by using response surface methodology. Desalin Water Treat. 2023;316:371–82. doi: 10.5004/dwt.2023.30207.
- [23] Albdiri ADZ, Mohammed AA, Hussein M, Koter S. Modeling of lead ions transport through a bulk liquid membrane. Desalin Water Treat. 2020;181:213–20. doi: 10.5004/dwt.2020.25098.

- [24] Ramesha K, Sudersanan PD, Santhosh N, Ravichandran G, Manjunath N. Optimization of friction stir welding parameters using Taguchi method for aerospace applications. In: Vinyas M, Loja A, Reddy K, edtiors. Advances in structures, systems and materials. Lecture notes on multidisciplinary industrial engineering. Singapore: Springer; 2020. p. 293–306. doi: 10.1007/978-981-15-3254-2 27.
- [25] Ramesha K, Sudersanan PD, Gowda AC, Santhosh N, Jangam S, Manjunath N. Friction stir welding of dissimilar aluminium alloys for vehicle structures. Int J Veh Struct Syst. 2022;14(1):5–9. doi: 10. 4273/ijvss.14.1.02.
- [26] El-Hofy M, Helmy MO, Escobar-Palafox G, Kerrigan K, Scaife R, El-Hofy H. Abrasive water jet machining of multidirectional CFRP laminates. Procedia CIRP. 2018;68:535–40. doi: 10.1016/j.procir. 2017.12.109.
- [27] Ramesha K, Santhosh N, Naresh H. Corrosion characterization of friction stir weld dissimilar aluminium alloy joints. J Mines Met Fuels. 2022;70(8A):16–22. doi: 10.18311/jmmf/2022/32003.
- [28] Kumar JP, Raj A, Ramesha K, Rout IS. Design and optimization of friction stir welding of Al-Cu BUTT joint configuration using Taguchi method. J Mines Met Fuels. 2022;70(8A):471–9. doi: 10.18311/jmmf/ 2022/32029.
- [29] Santhosh N, Praveena BA, Chandrashekar A, Mohanavel V, Raghavendra S, Basheer D. Wear behaviour of aluminium alloy 5083/SiC/fly ash inoculants based functional composites—optimization studies. Mater Res Express. 2022;9:076513. doi: 10.1088/ 2053-1591/ac8229.

- [30] Santhosh N, Praveena BA, Jain R, Hasan MA, Islam S, Khan MA, et al. Analysis of friction and wear of aluminium AA 5083/WC composites for building applications using advanced machine learning models. Ain Shams Eng J. 2022;14(9):102090. doi: 10.1016/j. asej.2022.102090.
- [31] Jagadeesan N, Selvaraj A, Nagaraja S, Abbas M, Ahamed Saleel C, Aabid A, et al. Response surface methodology based optimization of test parameter in glass fiber reinforced polyamide 66 for dry sliding, tribological performance. Materials. 2022;15(19):6520. doi: 10.3390/ma15196520.
- [32] Srikanth HV, Praveena BA, Arunkumar GL, Balaji S, Santhosh N, Sridhar K, et al. Production optimisation of mixed oil (rubber seed oil–fish oil) feedstock using response surface methodology and artificial neural network. Int J Ambient Energy. 2023;44(1):2336–46. doi: 10.1080/01430750.2023.2236107.
- [33] Lestari WD, Adyono N, Faizin AK, Haqiyah A, Sanjaya KH, Nugroho A, et al. Optimization of 3D printed parameters for socket prosthetic manufacturing using the taguchi method and response surface methodology. Results Eng. 2024;21(March 2024):101847. doi: 10.1016/j.rineng.2024.101847.
- [34] Santhana kumar M, Adalarasan R, Rajmohan M. Experimental modelling and analysis in abrasive waterjet cutting of ceramic tiles using grey-based response surface methodology. Arab J Sci Eng. 2015;40:3299–311. doi: 10.1007/s13369-015-1775-x.
- [35] Alberdi A, Suárez A, Artaza T, Escobar-Palafox GA, Ridgway K. Composite cutting with abrasive water jet. Procedia Eng. 2013;63:421–9. doi: 10.1016/j.proeng.2013.08.217.